RSC Advances

Bio-inspired Fabrication of Copper Oxide Nanowires Film with Switchable Wettability Via a Facile Method of Thermal Oxidation

Journal:	*RSC Advances*
Manuscript ID:	RA-ART-01-2015-000121.R1
Article Type:	Paper
Date Submitted by the Author:	17-Feb-2015
Complete List of Authors:	shi, yanlong; Hexi University, yang, wu; Northwest Normal University, feng, xiaojuan; hexi university, wang, yongsheng; hexi university, feng, lei; hexi university, yue, guoren; Hexi university,

Graphic

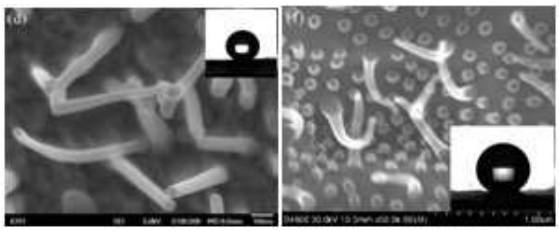

CuO nanowires surfaces imitating structures and superhydrophobicity of wings of boatman have been fabricated by thermal oxidation and surface modification.

Cite this: DOI: 10.1039/c0xx00000x

www.rsc.org/xxxxxx

ARTICLE TYPE

Bio-inspired Fabrication of Copper Oxide Nanowires Film with Switchable Wettability Via a Facile Method of Thermal Oxidation

YanLong Shi[a, b*], Wu Yang [b*], XiaoJuan Feng [a], Lei Feng [a], GuoRen Yue [a] and YongSheng Wang[b]

Received (in XXX, XXX) Xth XXXXXXXXX 20XX, Accepted Xth XXXXXXXXX 20XX

DOI: 10.1039/b000000x

CuO nanowires surface with micro/nanometer structures were constructed on copper substrate by a facile method of thermal oxidation, the CuO nanowires have similar micro/nanometer structures with hind wings of water boatman. The as-fabricated CuO nanowires surface is superhydrophilic, and the water contact angle on it is less than 5°. Modifying the CuO nanowires surface with dodecanethiol (DDT), and the wettability switched from superhydrophilicity to superhydrophobicity with the water contact angle of 154° and the glide angle of 4°. In addition, the original superhydrophilic behavior was regained via annealing at 300□ due to the desorbing of the low surface energy monolayer of DDT. The transition between superhydrophobicity and superhydrophilicity could be switched by alteration of adsorption/desorption of the monolayer of DDT. Compared with superhydrophilic CuO nanowires surface, the superhydrophobic CuO nanowires surface exhibits better corrosion resistance and self-cleaning property.

Introduction

In the past few years, the features of bio-inspired superhydrophobic surface have aroused worldwide attention because of its tremendous importance in fundamental research and potential applications in industries[1]. For a solid surface, when the water contact angle (CA) on it is larger than 150°, it is called superhydrophobic[2]. On the other hand, a surface with the water CA lower than 5°, it is called superhydrophilic[3]. Superhydrophobicity is a very important aspect of surface chemistry, which has many practical applications in self-cleaning[4], defrosting[5], anti-icing[6], anticorrosion[7], oil-water separation[8, 9], and microfluidic devices[10]. Inspired by the self-cleaning property of lotus leaf, which is originated from the micro/nanometer structures and chemical composition of low surface energy[11,12,13], many techniques were employed to construct water repelling surfaces, and the artificial fabrication of superhydrophobic surface becomes a hot area both in scientific and technological fields. Up to date, numerous superhydrophobic surface have been constructed on solid surfaces by creating micro/nanoscale binary structures and afterwards chemical modification with low surface energy materials[14]. There are many techniques to create hierarchical structures with micro/nanometer scale for the fabrication of superhydrophobicity on solid substrates, such as electrochemical deposition[15], chemical vapour deposition[16], electrospinning[17], hydrothermal reaction[18] and sol-gel[19], etc. In recent years, scientists have paid much attention to imitating the behaviours of creatures with special wettability. Jiang Lei etal investigated the efficient fog collection system of cactus *Opuntia microdasys*. Investigations show that the gradient of the Laplace pressure, the gradient of the surface-free energy and multi-function integration endow the cactus with an efficient fog collection system[20]. Furthermore, inspired by the novel fog collection system of cactus described above, they successfully developed an oleophilic array of conical needle structures for the collection of micro-sized oil droplets. Underwater, these structures mimic cacti can capture effectively micro-sized oil droplets and continuously transport them towards the base of the conical needles[21]. The other typical example is the discovery of the water-collecting ability of the capture silk of the cribellate spider *Uloborus walckenaerius*, after wetting, the "wet-rebuilt " fibres have characteristics of periodic spindle-knots, which are made of random nanofibrils. In addition, the fibres are separated by joints which are made of aligned nanofibrils. These structures features of fibres finally result in a surface energy gradient and a difference in Laplace pressure between the spindle-knots and the joints, the two factors act together to achieve continuous condensation and directional collection of water drops around spindle-knots. Based on the discovery, Zheng etal successfully designed artificial fibres which have similar structural features of silk, and realized the directional water-collecting function[22].

In our previously published literature, we reported the superhydrophobic behaviour of the hind wings of water boatman, which plays a crucial role in its swimming, balance keeping and escaping ability from water area under unfavourable conditions[23]. Inspired by the distinctive structures and excellent water repellency on the wings of water boatman, in this report, we have successfully fabricated CuO nanowires (NWs) film on copper substrate by thermal oxidation because of its technical simplicity and large scale growth capacity. The CuO NWs film has geometrical structures, and shows superhydrophobic behaviour

which is similar with wings of water boatman. In addition, the wettability conversion between superhydrophobicity and superhydrophilicity can be switched by alternation of surface modification and heat annealing. As for the wettability transition between superhydrophobicity and superhydrophiliciy, many techniques have been successfully employed to realize the wettability transition on copper substrate. For example, Zhang etal. fabricated a superhydrophobic surfaces on copper sheets by solution-immersion process and chemical modification with stearic acid. The reversibly switchable wettability transition between superhydrphobicity and superhydrophilicity could be controlled by the alternation of air-plasma treatment and stearic acid coating[24]. In addition, Liu etal. have fabricated a superhydrophobic surface on copper substrate by alternate current etching and modification of stearic acid, the reversible transition between superhydrophobicity and superhydrphilicity could be switched by annealing and remodification of stearic acid[25]. Furthermore, Zhang Tong-Yi. etal fabricated superhydrophilic CuO NWs surface on copper substrate by combining etching, electro-deposition and thermal oxidation, and the surface transited to be superhydrophobic after being exposed in air at room temperature for about 3 weeks, however, the pristine superhydrophilicity was recovered by dipping the sample into ascorbic acid solution[26]. The reversible transition between superhydrophobcity and superhydrophilicity controlled by alteration of exposing in air and dipping could be cycled at least four times. Compared with the common ways described above for fabricating reversible superhydrophilicity-superhydropbicity on copper substrate, the approach of thermal oxidation presented here is time-saving, low cost and simple, which may open a new avenue in the design and fabrication of switchable superhydrophobicity/superhydrophilicity on copper substrate.

Materials and Method

Chemicals

Copper plates with a purity of 99.9% were obtained from Shanghai Jinshan Chemical factory, China. Dodecanethiol was purchased form Beijing Chemical Works.

Fabrication of CuO nanorods film.

Copper plates with 1cm×2cm were ultrasonically degreased in acetone, absolute ethanol and distilled water for 10min, respectively. And then the plates were dried in an oven at 75□ for 10min. Later, copper plates were placed in a Muffle furnace at 400□ for 30min, finally, Muffle furnace was shut off and cooled to ambient temperature.

Surface modification.

Samples of CuO NWs films were immersed in an absolute ethanol solution of DDT (5wt%) for 24h, followed by washing in absolute ethanol and then drying in an oven at 75□ for 15min.

Characterizations.

X-ray photoelectron spectroscopy (XPS, PHI-5702) using with Al Ka radiation was employed to investigate the chemical states of superhydrophobic CuO NWs films. The crystal structure of CuO NWs film was characterized by a D/MAX-2400 (RIGAKU, Japan) X-ray diffractmeter with Cu Ka radiation. The surface morphologies of samples were observed by FE-SEM (JSM 6701F). Water contact angles on CuO NWs were measured by using contact angle meter (KRüSS, Germany) at room temperature, droplets of 8uL were placed at five different positions for one sample and the values were averaged.

Results and Discussion

Thermal oxidation is a typical method to fabricate CuO NWs directly on copper substrate. In this experiment, optically the surface of the copper substrate turns black in color after the thermal oxidation, indicating that the resultant is CuO, which is known to be black in colour. Fig1(a)-(d) show the surface morphologies of copper substrates oxidized at 400°for 30min. The low-magnification image(Fig 1a) shows a few CuO NWs are formed on the copper substrate. With the higher magnification image, we found that at the root of the CuO NWs, many convex polyhedral grains with diameters ranging from 50 to 200nm are observed, in addition, the CuO NWs, with length ranges from 0.1 ～1μm and the diameters are in the range of 40～60nm, are stuck out unevenly on numerous grain islands(as shown in Fig.1(b)-(c). Furthermore, with the highest magnification image, we can see that the CuO NWs with thick bottom and thin top structures are relatively smooth and aligned to the CuO grain islands. Just as described above, hierarchical structures of polyhedral grains and CuO NWs with micro/ nanometer scale were fabricated on copper substrates by thermal oxidation in air atmosphere.

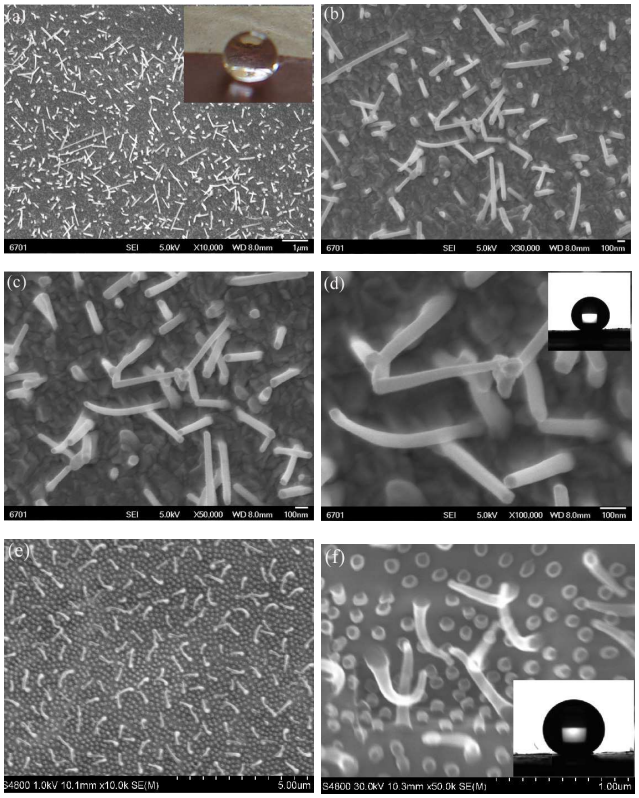

Fig. 1 (a-d)SEM images of CuO nanowires grown on substrate by thermal oxidation at 400□. (e-f) SEM images of hind wings of water boatman. The insets in Fig (a)-(d) and (f) are the images of water droplet on DDT-modified CuO nanowires and hind wing surface of boatman, respectively.

Thermal oxidation is the most common routine in the fabrication of CuO NWs, in the reaction process, the diameter and the length, as well as the structures of CuO NWs are

controlled by the annealing temperature, reaction time and the atmosphere in which a copper sample is oxidized[27]. According to Zhou etal report, three layers, inner Cu_2O grains layer, intermediate CuO grains and the top CuO NWs layer grown on CuO grains were formed in the reaction[28]. During the reaction process, when the oxidation temperature is up to 225 °C the formation of Cu_2O is favoured, while at higher temperatures that of CuO is favoured[29], and for the intermediate range of 300-400°C, CuO NWs growth occurs[28]. As for the growth mechanism of CuO NWs, vapour-solid (VS) or vapour-liquid-solid (VLS) mechanisms are usually employed to describe the growth process[30,31]. However, during the oxidation of copper substrate described here, CuO NWs were grown at relatively low temperature of 400℃, which is much lower than the melting points of both copper and its oxides, consequently, the equilibrium vapour pressures caused by copper or its oxides were negligibly small, therefore, the growth mechanism of CuO NWs can not be ascribe to any of these mechanism. Therefore, we believe the compressive stress-driven mechanism seems to be a plausible description for CuO NWs growth[28], which is detailed briefly as follows:

Cu ions diffuse to the outer surface of the stress-free CuO layer along the compressed grain boundaries (GBs) of CuO/Cu_2O interface due to the driving of the gradient of the chemical potential, which is induced by the gradient of the stress. Cu cation diffusing along the GBs are deposited on the top of grains via surface diffusion, which is driven by the concentration gradients of Cu ions between the GB junction area and at the root/tip of CuO NWs, where Cu ions are incorporated into the NWs growth via reacting with vapour oxygen in heating air. In the process, the compressive stress in the CuO layer is maintained due to the function of the solid-state phase transformation at the Cu_2O/CuO interface, this outward flux of Cu atoms continues and acts as a continual source of Cu cations for CuO NWs growth. The schematical illustration of CuO NWs grown on copper substrate by heat annealing in air is shown in Fig.2.

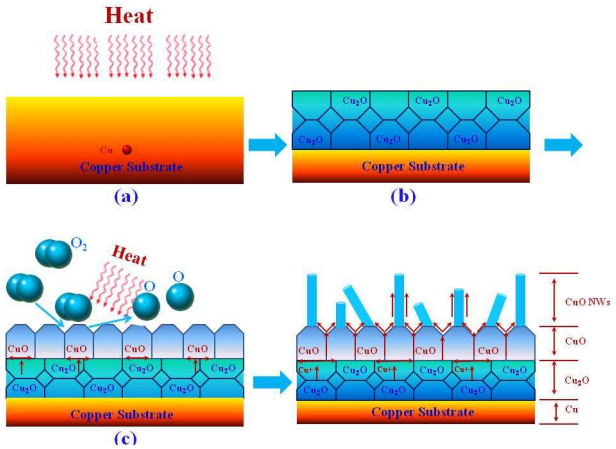

Fig. 2 Schematical illustration of the growth of CuO NWs on copper substrate

The hierarchical structures of CuO NWs fabricated by the thermal oxidation are similar with the hind wings of water boatman. In the published literature[23], we reported the hierarchical structures and superhydrophobic property of the hind wings of water boatman. Fig1(e-f) are SEM images of the hind wings of boatman, which revealed that the wings are composed of mastoids and NWs with diameters in the range of 80nm and 50-100nm, respectively. In addition, wings of insects are mainly composed of low surface energy materials of protein, lipid, and chitin, which are hydrophobic. Water contact angles on the wing surface were measured to be about 159° (as shown in the inset of Fig.1(f)) and the glide angle (GA) was about 8°. Superhydrophobicity of the hind wings of water boatman originates from the cooperation of hierarchical structures and hydrophobic materials. The superhydrophobicity of the wings enables water boatman to swim and breath freely in water with the assistance of trapped air in hind wings' surfaces, and to escape easily from water area under unfavourable conditions without being affected by moisture. The hierarchical structures of CuO NWs surface are similar with wings of boatman, however, the as-prepared CuO NWs surface is superhydrphilic and water droplets spread across quickly on the CuO NWs surface due to the construction of roughness could make a hydrophilic surface superhydrophilic and a hydrophobic surface superhydrophobic[32].

It is well known that the superhydrophobicity on solid surfaces is a synergistic effect of hierarchical micro/nanoscale binary structures combining low surface energy materials. The CuO NWs surface has similarly hierarchical structures with wings of water boatman, and we believe it is feasible to switch the wettability conversion of CuO surface from the initial superhydrophilicity to superhydrophobicity by decreasing the surface free energy. Therefore, samples of CuO NWs were immersed in a solution of DDT for 24h to decrease its surface free energy. After surface modification, CuO NWs surface could adsorb the low surface energy monolayer of DDT due to the following reactions[33, 35].

$$2RSH + 2CuO \longrightarrow (RS)_2 + Cu_2O + H_2O \quad (1)$$

$$2RSH + Cu_2O \longrightarrow 2RSCu + H_2O \quad (2)$$

As analyzed by the above chemical reactions, the monolayer of DDT is directly bonded with Cu atoms by forming a compound. The chemical bond is strong enough and can not be destroyed by washing, and more energy is needed to break the chemical bond (such as annealing), which will be discussed later in this report.

Before surface modification, the CuO NWs surface is superhydrophilic with a water CA less than 5°, however, the wettability was switched from superhydrophilic to superhydrophobic after being modified by DDT. The contact angle of water droplet on the superhydrophobic CuO surface is 154°(as shown in the insets of Fig 1(a) and (d)), and the GA is about 4°. The abrupt conversion from superhydrophilicity to superhydrophobicity further confirms the crucial role of hierarchical structures and chemical composition with low surface energy for the generation of superhydrophobicity.

As revealed above, for a solid surface, hierarchical structures and chemical composition with low surface energy are crucial to the formation of superhydrophobicity. Herein, the X-ray diffraction (XRD) patterns and X-ray photoelectron spectra (XPS) were employed to investigate the crystal structure and the chemical composition of CuO NWs. As shown in the XRD patterns (Fig 3a), except those diffraction peaks of copper marked

with triangles, all the indexed diffraction peaks (labelled as inverted triangles) can be indexed to the monoclinic phase of CuO .

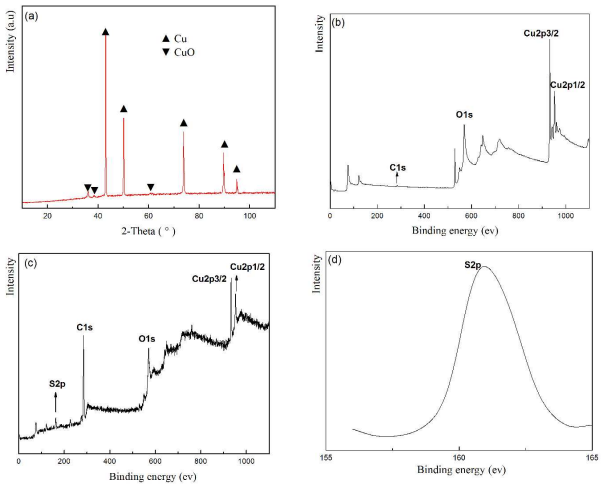

Fig. 3 (a) XRD pattern of CuO NWs, XPS of pristine (b) and DDT-modified(c-d) CuO NWs surface

The XPS spectra of CuO NWs surface before and after surface modification were shown in Fig 3(b-d). Before surface modification, the basic elements contained on pristine CuO NWs surface were surveyed by scanning bonding energy from 0 to 1100eV. Three characteristic peaks at 572.2, 933.9 and 952.4eV can be assigned to O1s, Cu2p3/2 and Cu 2p1/2, and the peak of C1s at 284.8 eV is almost invisible. However, with the surface modification, in addition to the peaks of C1s, O1s, Cu2p3/2 and Cu 2p1/2, characteristic peaks of S2p, S2s centered at of 163.2, 229.7eV were observed. Meanwhile, the corresponding content of element of S2p, O1s, C1s and Cu2p is 6.60%, 6.08%, 72.55%, and 14.78%, respectively. The characteristic peak of S2p and the sharply enhanced C1s peak confirms the monolayer of DDT assembled on CuO NWs surface[36] (as shown in Fig 3 (c) and (d)), which dramatically decrease the surface energy of CuO NWs surface. Consequently, chemical composition with low surface energy and hierarchical structures with micro/nanometer scale induced the formation of superhydrophobicity on CuO NWs surface.

As for the CuO NWs surface, the wettability was converted from superhydrophilic to superhydrophobic after being modified by DDT. However, for a plat copper substrate modified by DDT, it is hydrophobic and the CA is just about 103°. Herein, we employ Cassie-Baxter model to interpret the formation mechanism of superhydrophobicity on CuO NWs surface. According to the Cassie's theory[37], the superhydrophobic surface can be considered as a kind of porous medium composed of air pockets. When water droplets were dripped on the superhydrophobic CuO NWs surface, underneath the water droplets, air was trapped in the indentations between CuO grain islands or spaces among CuO NWs. In other words, the contacts between the water-droplet and the superhydrophobic CuO surface is a composite contact of solid-liquid-air, and water droplets sit mainly on air pockets and roll off easily when the surface is titled slightly. According to the following Cassie equation:

$$\cos\theta^* = f_1\cos\theta - f_2$$

Where θ is the CA of smooth Cu surface modified by DDT, θ=103°. θ* is the apparent CA of superhydrophobic CuO NWs surface, θ*=154°. f_1 and f_2 are the fraction of solid and air surfaces in contact with water droplets (ie., $f_1+f_2=1$), respectively. According the equation and the known values, f_2 and f_1 is roughly estimated to be about 87 % and 13 %, respectively. The results show that between the water droplets and the superhydrophobic CuO surface, the trapped air and CuO NWs respectively occupies about 87% and 13% of the composite contact area, as shown in Fig 4. Larger fraction of air (f_2) means larger CA and better superhydrophobicity, this further proves the fact that the hierarchical structures and the chemical composition with low surface energy accounts for the superhydrophobic behaviours of CuO NWs surface.

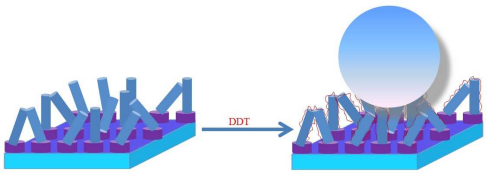

Fig. 4 Schematic illustration of formation of superhydrophobicity on CuO NWs surface

As described in published literature, roll-off behaviors of water droplets depend upon the metastable state energy and the barrier energy for a drop to move from one metastable state to another one[38]. Higher CA and lower GA indicates the superhydrophobic CuO NWs film possesses high metastable state energy and low barrier energy due to its dual scale decreases both the triple contact line and the wetted surface fraction[39]. When water droplets were dropped on the superhydrophobic CuO NWs film with a tilted angle of 4°, and found the droplets could roll off easily, which indicates the adhesion work between water droplets and superhydrophobic surface is quite small. The adhesion work can be roughly calculated by using the Young-Dupre equations described as follows[40,41,42].

$$W_{ad} = f_s \bullet \gamma_L(\cos\theta_Y + 1)$$

Where γ_L is the water surface tension, which is 7.2×10^{-3} N/m, θ_Y is the CA in Young model measured on a flat CuO surface, θ_Y =103°, and f_s is the surface fraction of CuO NWs in contact with water droplets, which is equals to f_1(f_1=13%) in Cassie-Baxter equation. With the known values of γ_L, θ_Y and f_s, W_{ad} is calculated to be about 7.25×10^{-4} N/m. The exceptionally small work of adhesion is responsible for the lower GA and self-cleaning.

Reversible Transition Between Superhydrophobicity and Superhydrophilicity

The pristine CuO NWs surface was superhydrophilic, and the CA was less than 5°, and water droplet spread out when water droplets were dripped on the surface. After surface modification by immersing the sample in DDT solution for 24h, the surface switched to be superhydrophobic with a water contact angle of

154°. Titling the superhydrophobic sample gently, the droplet could slide downwards as the titled angle approached 4°. However, the wettability of CuO NWs surface was switched from superhydrophobic to be superhydrophilic after being annealed at 300□ for 30min because the absorbed low surface energy material of DDT was desorbed by heat annealing. Immersed the annealed sample with superhydrophilicity in DDT solution again for 24h, the surface recovered its superhydrophobicity, and the contact angle did not change obviously. The reversible transition between superhydrophobicity and superhydrophilicity could at least cycle six times, as shown in Fig 5.

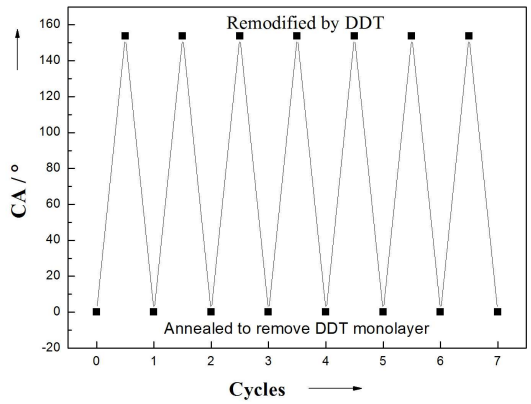

Fig. 5 Cycles between superhydrophilicity and superhydrophobicity of CuO NWs surface by alteration of modification and heat annealing.

Corrosion resistance

Potentiodynamic polarization curves were commonly employed to investigate the corrosion resistance of metals in 3.5wt% NaCl solution. The sample and a platinum stick were employed as the working and counter electrodes, respectively. A saturated calomel electrode (SCE) was used as reference electrode. Curves of a, b and c in Fig 6 show the potentiodynamic polarization curves of bare copper substrate, superhydrophilic and superhydrophobic CuO copper, respectively. The corresponding corrosion potential (E_{corr}) positively increased from -0.392V, -0.370V to -0.311V. In addition, the corrosion current density (i_{corr}) of superhydrophobic CuO substrate (3.136×10^{-6}A) decreased by more than 2 order of magnitude as compared to that of the bare copper substrate (1.171×10^{-4}A) or superhydrophilic (unmodified) CuO NWs substrate (1.087×10^{-4}A). In a typical polarization curve, a lower i_{corr} or a higher E_{corr} corresponds to a lower corrosion rate[43,44,45], and the shifts clearly show that superhydrophobic CuO surface presents the lowest corrosion rate, indicating the superhydrophobic CuO surface presents a good corrosion resistance property. It is believed that the air trapped in indentations between CuO grain islands behaves as a dielectric for a pure parallel plate capacitor[46]. Such an air dielectric can inhibit the electron transfer between the electrolyte and the CuO substrate and dramatically improve the corrosion resistance[7].

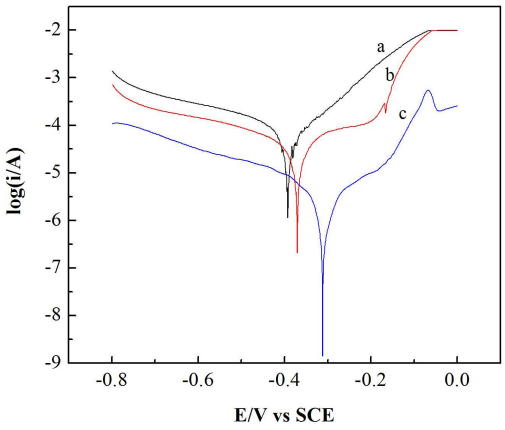

Fig. 6 Potentiodynamic polarization of curves of samples in neutral 3.5wt% NaCl solution. a, b, c separately corresponds to the sample of bare copper, superhydrophilic and superhydrophobic CuO NWs surface.

In addition to the corrosion resistance properties, the superhydrophobic CuO NWs film also exhibit self-cleaning property, which is similar with the lotus leaf. As we all know, water droplets can roll off the lotus leaf and completely carry away dust particles and surface contaminants spontaneously. Inspired by the simultaneous superhydrophobicity and low adhesion of lotus leaf, the self-cleaning property of the superhydrophobic CuO NWs film was investigated by sprinkling chalk powder as contaminants on its surface. Compared with the original superhydrophilic CuO NWs film, contaminants are more easy to be removed efficiently from the superhydrophobic surface by dripping water droplets on it (as shown in Fig 7(a)-(b)), which is similar with the typical property of louts leaf in nature.

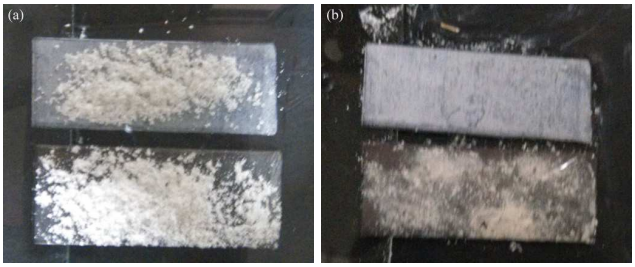

Fig. 7 Chalk powders on superhydrophobic (upper) and superhydrophilic (lower) CuO NWs surface before (a) and after water washing(b)

4. Conclusion

In conclustion, we have developed a simple means for mimicking nature by constructing a superhydrophilic CuO NWs surface via thermal oxidation, which has similar hierarchical structures with hind wings of water boatman. After surface modification, the surface exhibits similar water repellence (superhydrophobicity) with hind wings of water boatman with a contact angle of 154° and a gliding angle of ~4°. After annealing at 300℃ for 30min, the sample switched to be superhydrophilic again because of the absorbed DDT monolayer was desorbed, and the annealed sample recovered superhydrophobicity after being

re-modified by DDT. The reversible transition between superhydrophobicity and superhydrophilicity could at least cycle six times. Compared with the superhydrophilic surface, the superhydrophobic CuO NWs endows unique properties of corrosion resistance and self-cleaning. The method described here may offer a new strategy for the fabrication of reversible superhydrophobicity-superhydrophilicity material, which may be of great interest in biomimetic fabrication and industrial fields.

Acknowledgements

This work was supported by the National Natural Science Foundation of China (grant no. 20873101), the General Program of the Key Laboratory of Hexi Corridor Resources Utilization of Gansu Universities (grant no. ZX1406) and the President Fund of Hexi University(grant no. XZ201304).

Notes and references

[a]College of Chemistry and Chemical Engineering, Key Laboratory of Hexi Corridor Resources Utilization of Gansu Universities , HeXi University, Zhangye 734000, China. Fax: +86 09368282028. E-mail: yanlongshi726@126.com

[b]College of Chemistry and Chemical Engineering, Key Laboratory of Eco-Environmental Related Polymer Materials of MOE, Northwest Normal University, Lanzhou 730070, China.

Fax: +86 09317971216. E-mail: yangw@nwnu.edu.cn

† Electronic Supplementary Information (ESI) available: [details of any supplementary information available should be included here]. See DOI: 10.1039/b000000x/

‡ Footnotes should appear here. These might include comments relevant to but not central to the matter under discussion, limited experimental and spectral data, and crystallographic data.

1. Paul Roach, Neil J.Shirtcliffe and Michael I. Newton. *Soft Matter*, 2008, **4**, 224.

2. Didem Öner and Thomas J. McCarthy. *Langmuir*, 2000, **16**, 7777.

3. Rong Wang, Kazuhito Hashimoto, Akira Fujishima, Makoto Chikuni, Eiichi Kojima, Atsushi Kitamura, Mitsuhide Shimohigoshi and Toshiya Watanabe. *Advanced Materials*, 1998, **10**,135.

4. Xiao-Sheng Zhang, Fu-Yun Zhu, Meng-Di Han, Xu-Ming Sun, Xu-Hua Peng, and Hai-Xia Zhang. *Langmuir*, 2013, **29**, 10769.

5. Jonathan B. Boreyko, Bernadeta R. Srijanto, Trung Dac Nguyen, Carlos Vega, Miguel Fuentes-Cabrera, and C. Patrick Collier. *Langmuir*, 2013, **29**, 9516.

6. Min Ruan,Wen Li, Baoshan Wang, Binwei Deng, Fumin Ma, and Zhanlong Yu. *Langmuir*, 2013, **29**, 8482.

7. Lijun Liu, Feiyan Xu, and Lin Ma. *J. Phys. Chem. C*, 2012, **116**, 18722.

8. Paola Calcagnile, Despina Fragouli, Ilker S. Bayer, George C. Anyfantis, Luigi Martiradonna, P. Davide Cozzoli, Roberto Cingolani, and Athanassia Athanassiou. *ACS NANO*, 2012, **6**, 5413.

9. Xu Jin, Bairu Shi, Lichen Zheng, Xiaohan Pei, Xiyao Zhang, Ziqi Sun, Yi Du, Jung Ho Kim, Xiaolin Wang, Shixue Dou, Kesong Liu, and Lei Jiang. *Adv. Func. Mater*, 2014, **24**, 2721.

10. F. Shi, J. Niu, J. Liu, F. Liu, Z. Wang, X.-Q. Feng and X. Zhang. *Adv. Mater*, 2007, **19**, 2257.

11. W. Barthlott , C. Neinhuis. *Planta*, 1997, **202**, 1.

12. K. Liu , X. Yao , L. Jiang. *Chem. Soc. Rev*, 2010, **39**, 3240 .

13. Mingming Xiang, Anderson Wilhelm, and Cheng Luo. *Langmuir*, 2013, **29**, 7715.

14. L. Feng, S. Li, Y. Li, H. Li, L. Zhang, J. Zhai, Y. Song, B. Liu, L. Jiang and D. Zhu. *Advanced Materials,*2002, **14**,1857.

15. Manika Mahajan, Suresh K. Bhargava, Anthony P. O'Mullane. *Electrochimica Acta,* 2013, **101**, 186.

16. Xinwei Chen, Liang Hong, Yanfang Xu, and Zheng Wei Ong. *ACS Appl. Mater. Interfaces*, 2012, **4**, 1909.

17. Jing Wu, Nü Wang, Li Wang, Hua Dong, Yong Zhao, and Lei Jiang. *ACS Appl. Mater. Interfaces*, 2012, **4**, 3207.

18. Jun Zhang, Junyan Zhang. *Materials Letters*, 2013, **93**, 386.

19. Yu Yang, Yonghong Deng, Zhen Tong, and Chaoyang Wang. *ACS Sustainable Chem. Eng,* **2014**, ***2***, 1729.

20. Jie Ju, Hao Bai, Yongmei Zheng, Tianyi Zhao, Ruochen Fang, Lei Jiang. NATURE COMMUNICATIONS, 2012, 3,1247.

21. Kan Li, Jie Ju, Zhongxin Xue, Jie Ma, Lin Feng, Song Gao, Lei Jiang. NATURE COMMUNICATIONS, 2013, 4, 2276.

22. Yongmei Zheng, Hao Bai, Zhongbing Huang, Xuelin Tian, Fu-Qiang Nie, Yong Zhao, Jin Zhai, Lei Jiang. Nature, 2010, 463, 640.

23. Wang Y S, Shi Y L, Feng X J, Yang W, Yue G R. *Chin Sci Bull (Chin Ver)*, 2012. **57**. 1227.

24. Xiaotao Zhu, Zhaozhu Zhang , Xuehu Men , Jin Yang , and Xianghui Xu. *ACS Appl. Mater. Interfaces*, **2010**, ***2,*** 3636.

25. Zhiwei Wang , Liqun Zhu , Weiping Li , and Huicong Liu. *ACS Appl. Mater. Interfaces*, **2013**, ***5***, 4808.

26. Guoyong Wang, Tong-Yi Zhang. Journal of Colloid and Interface Science, 2012, 377, 438.

27. G Filipič and U Cvelbar. Nanotechnology, 2012, 23, 194001.

28. Lu Yuan, Yiqian Wang, Rediola Mema, Guangwen Zhou. Acta Materialia, 2011, 59, 2491.

29. G. Papadimitropoulos, N. Vourdas, V. Em. Vamvakas, D. Davazoglou. Thin Solid Films, 2006, 515, 2428.

30. Comini E, Baratto C, Faglia G, Ferroni M, Vomiero A, Sberveglieri G. Prog Mater Sci. 2009, 54,1-67.

31. Avramov I. Nanoscale Res Lett, 2007, 2, 235.

32. Wenzel R N, Ind Eng Chem, 1936, 28, 988.

33. H. Keller, P. Simak, W. Schrepp, J. Dembowski. *Thin Solid Film*, 1994, **244**, 799.

34. Myung M. Sung, Kiwhan Sung, Chang G. Kim, Sun S. Lee, and Yunsoo Kim. *J. Phys. Chem. B*, 2000, **104**, 2273.

35. Hannoch Ron, Hagai Cohen,Sophie Matlis, Michael Rappaport, and Israel Rubinstein. *J. Phys. Chem. B*, 1998, **102**, 9861.

36. Paul E. Laibinis, George M. Whitesides, David L. Allara, Yu-Tai Tao, Atul N. Parikh, and Ralph G. NUZZO. *J. Am. Chem. SOC,* 1991, ***113,*** 7152.

37. Cassie A B D, Baxter. S. *Trans Faraday Soc*, 1944, **40**, 546.

38. Gross, M.; Varnik, F.; Raabe, D.; Steinbach, I. *Physical Review E*. 2010, **81**, 051606.

39. Gao, L. C.; McCarthy, T. J. *Langmuir*, 2006, **22**, 6234.

40. Schrader, M. E. *Langmuir*, 1995, **11**, 3585.

41. Xiu, Y.H.; Zhu, L.B.; Hess, D. W.; Wong, C. P. *J. Phys. Chem. C*, 2008, **112**, 11403.

42. Kim, J.Y.; Kim, E.K.; Kim, S.S. *Journal of Colloid and Interface Science*, 2013, **392**, 376.

43.Takahiro Ishizaki and Michiru Sakamoto. *Langmuir*, 2011, **27**, 2375.

44.Takahiro Ishizaki, Yoshitake Masuda, and Michiru Sakamoto. *Langmuir*, 2011, **27**, 4780.

45. Lijun Liu, Feiyan Xu, Zhenlin Yu,Ping Dong. *Applied Surface Science*, 2012, **258**, 8928.
46. Peng Wang, Dun Zhang, Ri Qiu, Baorong Hou. *Corrosion Science*, 2011, **53**, 2080.